Available online at www.sciencedirect.com
ScienceDirect
Infection, Genetics and Evolution 8 (2008) 205–212
Infection, Genetics and Evolution
www.elsevier.com/locate/meegid

Short communication

Phylogenetic and structural information on glyceraldehyde-3-phosphate dehydrogenase (G3PDH) in *Plasmodium* provides functional insights☆

Sheila Akinyi [a], Jenny Gaona [b], Esmeralda V.-S. Meyer [a], John W. Barnwell [c], Mary R. Galinski [a,d], Vladimir Corredor [a,b,*]

[a] *Emory Vaccine Center, Yerkes National Primate Research Center, Emory University, 954 Gatewood Road, Atlanta, GA 30329, USA*
[b] *Unidad de Parasitolgía, Departamento de Salud Pública, Facultad de Medicina, Universidad Nacional de Colombia, Bogotá, Colombia*
[c] *Division of Parasitic Diseases, National Center for Infectious Diseases, Centers for Disease Control, Atlanta, USA*
[d] *Department of Medicine, Division of Infectious Diseases, Emory University, 954 Gatewood Road, Atlanta, GA 30329, USA*

Received 19 August 2007; received in revised form 10 October 2007; accepted 12 October 2007
Available online 22 October 2007

Abstract

Plasmodium is dependent on glycolysis for ATP production. The glycolytic enzyme glyceraldehyde-3-phosphate dehydrogenase (G3PDH) plays an important role in glycolysis and is, therefore, a potential target for antimalarial drug development. The *g3pdh* gene of nine *Plasmodium* species was sequenced from genomic DNA and the type and origin determined by phylogenetic analysis. Substitutions were analyzed over a wide phylogenetic spectrum in relation to the known three-dimensional structures of the *P. falciparum* and human proteins. Substitutions were found within the functional domains (Rossman NAD+-binding and catalytic domains). A number of replacements within the adenosyl-binding surfaces were found to be conserved within the Chromoalveolates, others in the Apicomplexa, and still others within the genus *Plasmodium*, all of which were different from the human sequence. These sites may prove to be of functional importance and provide insights for drug-targeting studies, as have other regions examined in *Leishmania* and *Toxoplasma* G3PDH research.

Keywords: Glyceraldehyde-3-phosphate dehydrogenase; Apicomplexa; *Plasmodium*; Glycolysis; Phylogenetic tree; Catalytic domain; NAD+-binding domain; Drug discovery

1. Introduction

Plasmodium parasites cause more than one million deaths and sicken 300–500 million people with malaria infections each year (Roll Back Malaria (RBM) and (WHO), 2005). The discovery of new drug targets is a global priority to help combat the spread of drug-resistant parasites (Biot and Chibale, 2006; Newton and White, 1999). Glyceraldehyde-3-phosphate dehydrogenase (G3PDH) is an essential enzyme in *Plasmodium* and recent crystallographic studies suggest it can be a target for therapeutic intervention (Robien et al., 2006; Satchell et al., 2005).

When *Plasmodium* parasites invade red blood cells (RBCs), they must provide their own molecular machinery to support growth and development, and in essence remodel the infected host cell (Roth et al., 1988). Mature RBCs have been referred to as ''floating corpses'' due to their lack of nuclei, protein synthesis capabilities and trafficking machinery (Gratzer, 1984). To achieve its needs, the intraerythrocytic *Plasmodium* is heavily dependent on glycolysis for the production of ATP, as illustrated by the much higher glycolytc activity of parasitized RBCs over uninfected ones (Roth, 1990; Roth et al., 1988). This is of particular importance given that the parasite seems to lack a complete tricarboxylic acid cycle in its asexual stages due to the absence of a pyruvate dehydrogenase complex (Foth et al., 2003; Sherman, 1998).

G3PDH is a homotetrameric enzyme with dihedral symmetry consisting of two major functional domains: the Rossman N-terminal NAD+ cofactor-binding domain and the C-terminal catalytic domain (Daubenberger et al., 2000; Nagradova, 2001). The crystal structure of the *P. falciparum*

☆ *Note*. Nucleotide sequence data reported in this paper are available in the GenBank, EMBL and DDBJ databases under the accession number(s): EU045402, EU045403, EU045404, EU045405, EU045406, EU045407, EU045408, EU045409, EU045410.

* Corresponding author.
E-mail address: vcorred@emory.edu (V. Corredor).

1567-1348/$ – see front matter © 2007 Elsevier B.V. All rights reserved.
doi:10.1016/j.meegid.2007.10.003

G3PDH has been solved at 2.25 Å (Robien et al., 2006) and 2.6 Å (Satchell et al., 2005) resolution revealing that NAD+ binds to one of each of the four subunits on the G3PDH tetramer and that with the exception of a bulge, created by the so-called S-loop, that separates the NAD+-binding cavities of adjacent subunits, the structure is very similar to the human G3PDH. The S-loop is structurally different from the human sequence and in close proximity to the catalytic site, and hence it is considered as a potential drug target site. Sequence similarity between *P. falciparum* G3PDH and human G3PDH is about 63.5% (Daubenberger et al., 2000).

There are greater than 5000 known species within the phylum Apicomplexa, which includes the clinically relevant parasites *Plasmodium*, *Toxoplasma*, *Cryptosporidium*, *Eimeria* and *Babesia* (Rich and Ayala, 2003; Waller et al., 1998). In addition to the glycolytic function, there is evidence in some species including humans and fungi that cytosolic G3PDH may have non-glycolytic functions associated with membrane fusion, microtubule bundling, nuclear RNA export, DNA repair, apoptosis, and cell adhesion (Barbosa et al., 2006; Colell et al., 2007; Sirover, 1999). Evidence also exists showing that *P. falciparum* G3PDH may play a role in apical complex biogenesis (Daubenberger et al., 2003) and this activity is inhibited by the hemoglobin degradation product, ferriprotoporphyrin IX (Campanale et al., 2003). The N-terminus of *P. falciparum* G3PDH has been shown to interact with the GTPase Rab2 and mediate its recruitment to microsomal membranes in a HeLa cell experimental system (Daubenberger et al., 2003). These data support the proposition that *Plasmodium* G3PDH may have acquired multiple functions during its course of evolution, and underscores the importance of G3PDH in the survival of malaria parasites.

In *P. falciparum* the enzyme is encoded by a single copy, two-exon, 1.3 kb gene that is transcribed in ring, trophozoite and schizont stage parasites. It is maximally expressed in early developing schizonts and the RNA levels are reduced in late stage schizonts (Daubenberger et al., 2000; Bozdech et al., 2003; our unpublished data).

The conserved albeit evolutionarily distinct G3PDH enzymes present in humans, *Plasmodium* and other Apicomplexa have slightly differing structures that could be targeted for the development of specific inhibitors and may provide a means for therapeutic intervention for malaria infections (Brady and Cameron, 2004; Dobeli et al., 1990; Wanidworanun et al., 1999). This strategy has had success in drug-targeting studies involving *Trypanosoma* and *Leishmania* G3PDH where adenosine analogs have been developed and function as selective inhibitors of *Trypanosoma* G3PDH (see Lakhdar-Ghazal et al., 2002; Opperdoes and Michels, 2001, for reviews). The availability of the crystal structure of *P. falciparum* G3PDH (Robien et al., 2006; Satchell et al., 2005) allows for a detailed comparison of G3PDH sequences and structures in *Plasmodium*, with other Apicomplexa, and humans.

In this study, the *g3pdh* gene from various *Plasmodium* species was sequenced and a comparative analysis performed. The aim was to identify amino acid substitutions in the *Plasmodium* G3PDH protein that may reveal residues of potential functional importance (including functions other than glycolysis), distinct from the human host and thus provide insights for future experimentation and the development of therapeutic interventions.

2. This study

To advance research in this direction, the type and origin of *g3pdh* in *Plasmodium* was determined through a phylogenetic analysis that included 12 *Plasmodium* species and sequences from 110 species along a wide phylogenetic spectrum. Then, the pattern of substitutions that differed between the human and *Plasmodium* sequences was analyzed within the framework of an alignment covering *g3pdh* sequences from diverse species within the ''supergroup'' Chromalveolates, including members of the Apicomplexa (Figs. 1 and 2). In addition to including several available published *Plasmodium g3pdh* sequences, the *g3pdh* gene was cloned and sequenced from a number of additional *Plasmodium* species and additional strains: the human species *P. falciparum* (FVO), *P. vivax* (Salvador I), and *P. malariae* (Uganda 1), the chimpanzee species *P. reichenowi* (CDC1), and the simian species *P. knowlesi* (H strain), *P. coatneyi* (Type strain), *P. cynomolgi* (Berok), *P. brasilianum* (Peru II), *and P. fragile* (Nilgiri), using purified genomic DNA that had been preserved from primate blood-stage infections.

Standard PCR amplifications were performed using *g3pdh*-specific primers (Table 1) and the Roche High Fidelity System (Roche, Indianapolis, IN) and KOD HotStart DNA Polymerase (Novagen, San Diego, CA) with the following conditions: 30 cycles of denaturation (94 °C, 1 min), annealing (48 °C, 1 min) and extension (68 °C, 2.5 min). Two independent rounds of PCR amplification and sequencing were performed. All PCR products were purified using the QIAquick PCR purification kit (Qiagen, Valencia, CA) and cloned into the pCR2.1-TOPO vector. Purified plasmid DNA from 10 positive clones was sequenced using BigDye Terminator v. 3.1 Cycle sequencing kit (Applied Biosystems, Foster City, CA). The sequences were assembled and aligned using the MacVector software package CLUSTALW and refined manually.

A *g3pdh* sequence database was built using new and published *Plasmodium* sequences as well as *g3pdh* sequences

Table 1
List of oligonucleotides used in this study

Name	Sequence
VC25F	5′-ATT AAT GGA TTT GGT CGT ATC-3′
VC24R	5′-CAA GTA CAC GGT TTG AGT ATC-3′
PfGP44F	5′-GAC GTT TAG TAT TTA GAG C-3′
PfGP366F	5′-TGC TAT CTC TTG AAA TAC-3′
PfGP507F	5′-CAA GTA GAT GTT GTA TGT-3′
PfGP534R	5′-CAG TTG ATT CAC ATA CAA-3′
PfGP1230R	5′-TAG TTG TTA GTA ATG TGT AC-3′
PvGP450F	5′-ACT TGT GCT ACT TGC TCA-3′
PmGP566F	5′-CTA CTA GCG TAC GAC TC-3′
PbrGP484F	5′-CTA CTA GCG TAC GAC TCA-3′
PbrGP361F	5′-GAG TAT GTT CAT GCA GTT-3′
PcoGP454F	5′-AGC ACT TGT GTT ACT TGC-3′
PcyGP467R	5′-TTG CAA TTG GAG CTA AAC-3′

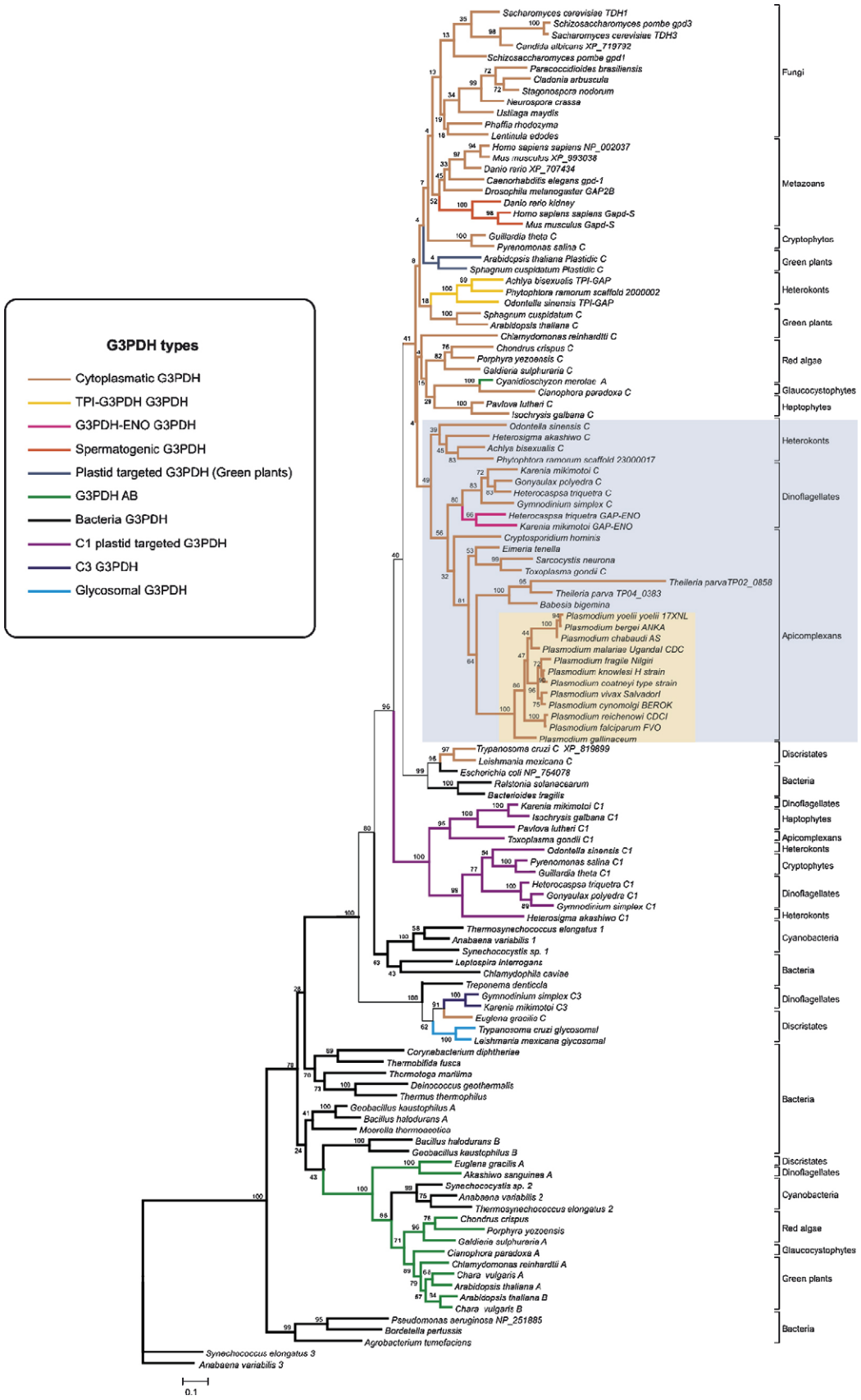

Fig. 1. Maximum likelihood tree of G3PDH. Bootstrap values are indicated above the branches. Branch lengths are the number of substitutions per site according to the scale. G3PDH types are indicated by color branches, Chromoalveolates are highlighted in grey and the *Plasmodium* genus is indicated in brown.

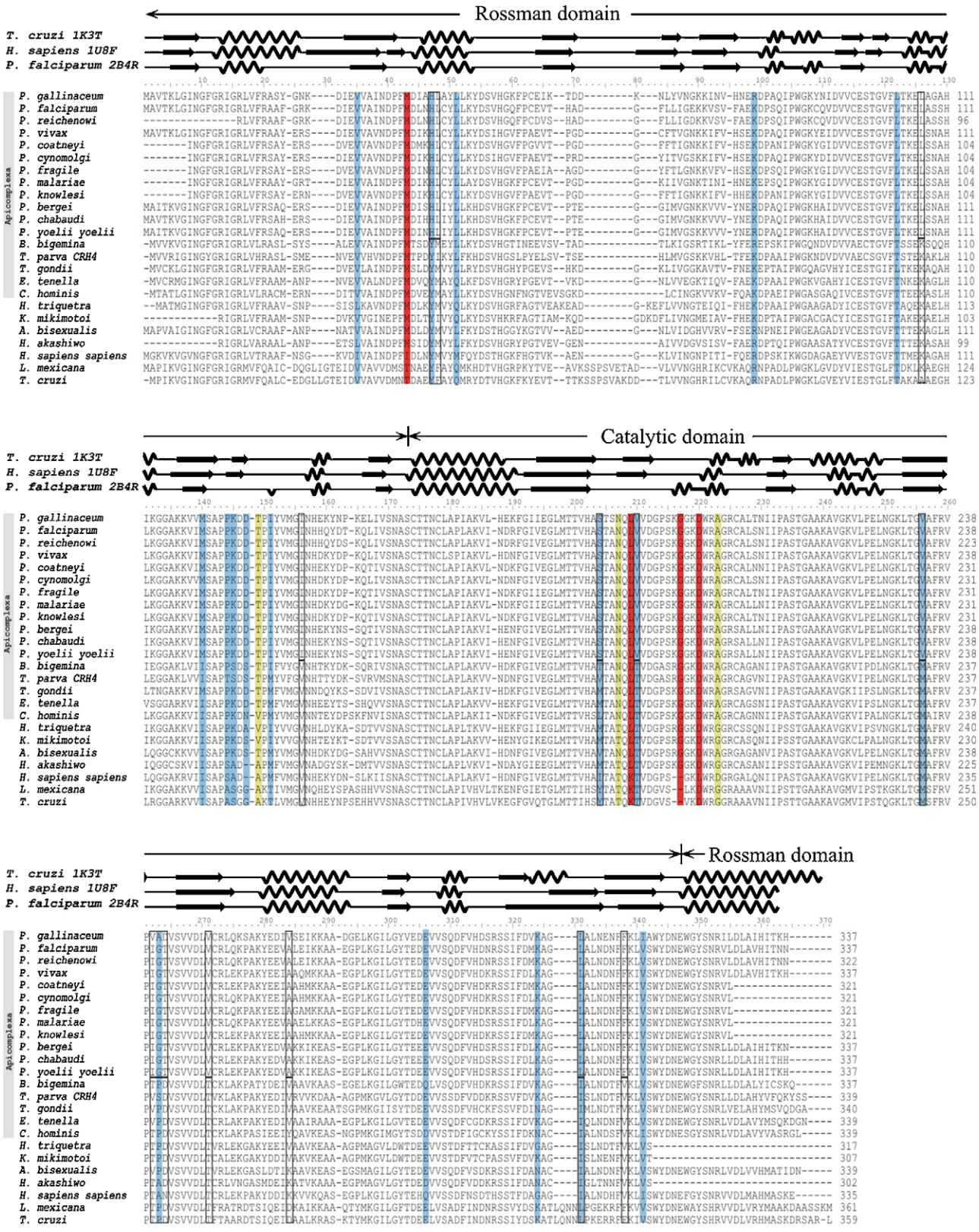

Fig. 2. Amino acid sequence alignment of the functional domains of G3PDH—the Rossman NAD+-binding and catalytic domains. The alpha helix (∼∼) and beta sheet (→) secondary structures are indicated on top of the alignment. Substitutions that are conserved in Chromalveolates (red box), Apicomplexa (yellow) or *Plasmodium* (blue) but different from the human sequence and part of the NAD-binding pocket surface are shown. In addition, the figure shows replacements that are unique to *Plasmodium* species (boxed residues).

Table 2
List of species, identification numbers and database of origin for the sequences used in this study

Species/strain	Sequence ID	Database
P. falciparum 3D7	PF14_0598	PlasmoDB 3.5
P. falciparum FVO	EU045404 (this study)	GenBank
P. reichenowi CDC1	EU045408 (this study)	GenBank
P. knowlesi H strain	EU045406 (this study)	GenBank
P. coatneyi Type strain	EU045403 (this study)	GenBank
P. cynomolgi Berok	EU045409 (this study)	GenBank
P. vivax Salvador I	EU045410 (this study)	GenBank
P. fragile Nilgiri	EU045405 (this study)	GenBank
P. brasilianum Peru II	EU045402 (this study)	GenBank
P. malariae Uganda 1	EU045407 (this study)	GenBank
P.y. yoelli	PY03280	PlasmoDB 3.5
P. berghei	PB000084.03.0	PlasmoDB 3.5
P. chabaudi	PC000143.05.0	PlasmoDB 3.5
P. gallinaceum	Pgal1137d09.q1k	Sanger P. gallinaceum Genome Project
	Pgal1137b01.q1k	Sanger P. gallinaceum Genome Project
	Pgal0998b08.p1k	Sanger P. gallinaceum Genome Project
	Pgal1137d09.p1k	Sanger P. gallinaceum Genome Project
	Pgal0362b01.p1k	Sanger P. gallinaceum Genome Project
	Pgal0373g08.q1k	Sanger P. gallinaceum Genome Project
	Pgal1128h02.p1k	Sanger P. gallinaceum Genome Project
	Pgal0647a02.p1k	Sanger P. gallinaceum Genome Project
	Pgal0547d07.q1k	Sanger P. gallinaceum Genome Project
B. bigemina	Contig4141.0	Sanger Babesia bigemina genome project
B. bovis	chr*2*924*18	TIGR Babesia bovis genome project
T. parva	AAGK01000004	GenBank
	AAGK01000002	GenBank
T. annulata	TA15530_chr2	Sanger Theileria annulata genome project
	TA08145_chr4	Sanger Theileria annulata genome project
C. parvum	AAEE01000002	CryptoDB 3.4
C. hominis	AAEL01000124	CryptoDB 3.4
E. tenella	Et_v1_Twnscn_ Contig12652.tmp3	Sanger Eimeria tenella genome project
N. caninum	TC3080 TC1626	USDA-WashU Neospora EST Project
S. neurona	TC2288 TC1094 TC1379 TC479	USDA-WashUgene index project
T. gondii	80.m00003	ToxoDB 4.1
	IX-4-3473658-3472567	
	59.m00091	ToxoDB 4.1
	VIII-4-5999894-5998908	
H. triquetra	AB195834	GenBank
	AB106701	GenBank
	AB106700	GenBank
G. polyedra	AF028560	GenBank
	AF028562	GenBank
G. simplex	AB106693	GenBank
	AB106694	GenBank
	AB106695	GenBank
A. sanguinea	AB106697	GenBank
	AB106696	GenBank
K. mikimotoi	AB164183	GenBank
	AB164184	GenBank
	AB164185	GenBank
	AB164186	GenBank
O. sinensis	AF063800	GenBank
	AF063801	GenBank
	AF063802	GenBank
H. akashiwo	AF319448	GenBank
	AF319449	GenBank
A. bisexualis	AF063107	GenBank
	AF063106	GenBank
P. ramorum	scaffold_ 23000017	DOE Joint Genome Institute. Phytophthora ramorum V1.1
	scaffold_ 2000002	DOE Joint Genome Institute. Phytophthora ramorum V1.1
P. lutheri	AY292376	GenBank
	Cluster Id PLL00000015	TBestDB
I. galbana	Cluster Id ISL00000338	TBestDB
	Cluster Id ISL00001421	TBestDB
G. theta	U40032	GenBank
	U39873	GenBank
P. salina	U40033	GenBank
	U39897	GenBank
C. albicans	XM_714816	GenBank
	XM_714699	GenBank
S. cerevisiae	S000003588	Saccharomyces genome database
	S000003769	Saccharomyces genome database
	S000003424	Saccharomyces genome database
S. pombe	NM_001021142	GenBank
	NM_001022073	GenBank
P. brasiliensis	AF396657	GenBank
C. arbuscula	AY170750	GenBank
S. nodorum	AJ271155	GenBank
N. crassa	XM_951884	GenBank
U. maydis	X07879	GenBank
P. rhodozyma	AF006483	GenBank
L. edodes	AB012862	GenBank
D. melanogaster	NM_080352	GenBank
	NM_001038847	GenBank

Table 2 (*Continued*)

Species/strain	Sequence ID	Database
C. elegans	NM_076134	GenBank
	NM_063836	GenBank
	NM_076133	GenBank
	NM_063791	GenBank
D. rerio	BC066528	GenBank
	XM_702342	GenBank
M. musculus	XM_987944	GenBank
	NM_008085	GenBank
H. sapiens	NM_002046	GenBank
	NM_014364	GenBank
T. cruzi	XM_814806	GenBank
	XM_810475	GenBank
L. mexicana	X65226	GenBank
	X65220	GenBank
E. gracilis	L21904	GenBank
	L39772	GenBank
A. thaliana	NM_103456	GenBank
	NM_101161	GenBank
	NM_101214	GenBank
	NM_101496	GenBank
	NM_106601	GenBank
	NM_111283	GenBank
	NM_113576	GenBank
S. cuspidatum	AJ246022	GenBank
	AJ246021	GenBank
	AJ246031	GenBank
	AJ246032	GenBank
C. vulgaris	AJ246015	GenBank
	AJ246016	GenBank
	DQ270262	GenBank
	AJ246014	GenBank
C. reinhardtii	L27669	GenBank
	L27668	GenBank
C. crispus	X73033	GenBank
	X73036	GenBank
P. yezoensis	AY273819	GenBank
	AY273820	GenBank
G. sulphuraria	AJ012286	GenBank
	contig951	The *Galdieria sulphuraria* Genome Project
C. merolae	c10f0002	*Cyanidioschyzon merolae* Genome Project
	c13f0002	*Cyanidioschyzon merolae* Genome Project
	c10f0010	*Cyanidioschyzon merolae* Genome Project
C. paradoxa	AJ313316	GenBank
	DQ270258	GenBank
E. coli	NP_753744	GenBank
	NP_754078	GenBank
R. solanacearum	NP_520870	GenBank
B. fragilis	YP_098251	GenBank
T. elongatus	NP_680834	GenBank
	NP_682256	GenBank
	NP_682731	GenBank
A. variabilis	YP_321014	GenBank
	YP_324215	GenBank
	YP_322831	GenBank
Synechocystis sp. PCC 6803	NP_440929	GenBank
	NP_442821	GenBank
L. interrogans	NP_711885	GenBank
C. caviae	NP_828990	GenBank
T. denticola	NP_972094	GenBank
C. diphtheriae	NP_939663	GenBank
T. fusca	YP_290073	GenBank
T. maritima	NP_228497	GenBank
D. geothermalis	YP_604599	GenBank
T. thermophilus	YP_004524	GenBank
G. kaustophilus	YP_148579	GenBank
	YP_148911	GenBank
B. halodurans	NP_244015	GenBank
	NP_244427	GenBank
M. thermoacetica	YP_429140	GenBank
P. aeruginosa	NP_249242	GenBank
	NP_251691	GenBank
	NP_251885	GenBank
B. pertussis	NP_879794	GenBank
A. tumefaciens	AAL44547	GenBank

from other eukaryotes (Table 2). Protein sequences were aligned according to G3PDH type groups with 3DCoffee (O'Sullivan et al., 2004), using available G3PDH crystal structures as a reference. Secondary structure predictions (obtained by DSSP) were drawn over the alignments using the Structural Alignment Package, STRAP (Gille and Frommel, 2001). Position assignment to protein surfaces was achieved using the Computed Atlas of Surface Topography of proteins (Binkowski et al., 2003). The designation of ambiguous positions and alignment refinements were carried out by eye using Bioedit 7.1.2 (Hall, 1999) and the outputs from 3DCoffee and STRAP as a guide. A phylogenetic tree was reconstructed using maximum likelihood methods using the PHYML V2.4.3 program (Guindon et al., 2005). The best substitution model and its parameter values were obtained using ProtTest (Abascal et al., 2005). A phylogenetic tree was reconstructed under the WAG + I evolutionary model; gamma distribution was calculated using four rate categories, pinv 0.05, alfa 0.86 and homogeneous rates across the tree. Bootstrap values over 500 replicates are indicated on each branch in percentage values.

The phylogenetic tree in Fig. 1 was built to determine the origin and identity of the *Plasmodium g3pdh* gene. Fig. 1 shows that both cytosol- and plastid-targeted G3PDH of Chromalveolates (Heterokonts and Alveolates) are of eukaryotic origin, as previously noted (Fast et al., 2001). Similar results with slightly different topologies are obtained with the Bayesian and NJ methods (data not shown). Positions homologous to D32, L187, P188 of the *S. stearothermophilus* G3PDH sequence (M24493), which are involved in the specific binding of NAD+ to the enzyme, allow for the classification of G3PDH sequences as plastid-targeted (NADP+) or cytosol-targeted enzymes (NAD+). The corresponding positions were checked in the G3PDH sequences of all taxa in this study and all *Plasmodium* G3PDH sequences analyzed were found to be compatible with a cytosolic classification. Fig. 1 also shows that the origin of *Plasmodium g3pdh* sequences is monophyletic.

A representative alignment of the Chromalveolates (Fig. 2) reveals 117 amino acids within the functional Rossman and catalytic domains that are conserved. Constraints in G3PDH

within the *Plasmodium* lineage follow the same general pattern of G3PDH sequences compared across different phylogenetic lineages; i.e., the catalytic domain is more conserved than the Rossman domain. When the human and *Plasmodium* sequences are compared, most variable sites are located within the Rossman domain (68%). In contrast the catalytic domain contains fewer variable sites (30%). Constraints in the catalytic domain are mainly due to the way the substrate interacts with the holoenzyme: glyceraldehyde-3-phosphate and cysteine 174 interact to form a covalent hemithioacetal intermediate which is then oxidized to a thioester. NAD+ bound to the enzyme acts as the receptor of a hydride ion and is reduced to NADH. This reaction is facilitated by the conserved histidine 202 residue in the active site followed by a phosphorolytic attack on the thioester by inorganic phosphate that releases the final 1,3-bisphosphoglycerate product. Therefore, the adenosyl-binding pocket surface may constitute an obvious target for drug development.

Twenty-five sites at the NAD-binding pocket surface, as determined using the CASTp program (Binkowski et al., 2003), display variation between the human and *Plasmodium* sequences. Sites conserved along different phylogenetic spectra (i.e. Chromalveolates, Alveolates, Apicomplexa or the *Plasmodium* lineages) and which are therefore assumed to represent different functional constraints, may represent attractive target sites. Four sites (Fig. 2; shaded in red) are conserved in the Chromalveolates. Three (L209, G217 and D220) are located in the so-called S-loop near the catalytic site and residue 216, also within the S-loop, has only two morphs (a conservative substitution R → K). Of those, site 220 is only variable in the human sequence (a hydrophobic small amino acid versus a hydrophilic small amino acid) and therefore seems to be highly constrained in the Chromalveolate lineage. Two positions (Fig. 2; shaded in yellow) are conserved in the Apicomplexa lineage (N207 and A223) and are close or within the S-loop and represent attractive targets for functional studies.

Fifteen substitutions (or 17 if excluding *P. gallinaceum*) are conserved within the *Plasmodium* lineage (Fig. 2, shaded in blue) within the NAD-binding surface. Substitutions Y47, R/K99, P144, K145 and G263 are of particular interest. In the *P. falciparum* protein Y47 makes a hydrogen bond with S215, R99 binds NAD+ via a carbonyl oxygen, P144 and K145 are close to the active site, and G263 may be part of a surface thought to possibly bind the small molecule CGP-3466 that inhibits the pro-apoptotic G3PDH activity in human cells (Jenkins and Tanner, 2006). While many sites conserved within *Plasmodium* may allow for a variety of substitutions in other phylogenetic groups, a few sites are only dimorphic (H47, R/K99, V210, L122, K216, M256, V341) suggesting greater constraints. These dimorphic sites could be considered for their potential as additional inhibitory targets, but also as sites worth probing experimentally from a functional perspective. It is of value to note that a KG insertion within the S-loop previously observed in *P. falciparum* is conserved in all *Plasmodium* species (K216, G217; Fig. 2) and the Chromalveolates, further increasing the potential importance of this site as a possible drug target.

Fourteen replacements are unique to mammalian-infecting *Plasmodium* species—H47, L48, L126, I156, S204, V210, V256, I262, G263, T264, V271, A284, L331 and F338. Of those, H47, S204, V210, V256, G263 and L331 are part of the NAD-binding surface. Residues I262 and T264 are part of the central channel formed in the quaternary structure by the assembly of all four monomers.

One would expect that the wider the phylogenetic spectrum being analyzed, the fewer the number of conserved substitutions. Interestingly, when analyzing conserved G3PDH residues that differ from the human sequence within large taxonomic divisions, the majority of them fall into the adenosyl-binding pocket. For example, there are 113 conserved sites between the human sequence and the Chromalveolates and 117 conserved sites in the Chromalveolates, of the four variable residues between the human sequence and the Chromalveolates three are part of the adenosyl pocket, further increasing the interest of those residues from a functional point of view.

3. Conclusion

This analysis shows that G3PDH in *Plasmodium* is monophyletic and of the cytosolic type. It contains residues with potential functional importance that can be experimentally probed and may eventually constitute appropriate targets for drug development. One hundred and thirty-three positions were identified within the two functional (Rossman NAD+-binding and catalytic) domains that are conserved within the Apicomplexa. Some of these residues are part of the NAD+-binding pocket surface, and as a consequence may be of functional importance: four are conserved in the Chromalveolates, and two within Apicomplexa, while 15 are conserved among *Plasmodium* species. Also of interest are five amino acid substitutions within this surface that are uniquely conserved among *Plasmodium* species. Drug design for malaria and other pathogens has the challenge of designing specific inhibitors that do not affect the function of counterpart proteins present in humans. This study reveals unique amino acid substitutions within functionally important sites that provide attractive targets for therapeutic intervention.

References

Abascal, F., Zardoya, R., Posada, D., 2005. ProtTest: selection of best-fit models of protein evolution. Bioinformatics 21, 2104–2105.

Barbosa, M.S., Bao, S.N., Andreotti, P.F., de Faria, F.P., Felipe, M.S., dos Santos Feitosa, L., Mendes-Giannini, M.J., Soares, C.M., 2006. Glyceraldehyde-3-phosphate dehydrogenase of *Paracoccidioides brasiliensis* is a cell surface protein involved in fungal adhesion to extracellular matrix proteins and interaction with cells. Infect. Immun. 74, 382–389.

Binkowski, T.A., Naghibzadeh, S., Liang, J., 2003. CASTp: computed atlas of surface topography of proteins. Nucleic Acids Res. 31, 3352–3355.

Biot, C., Chibale, K., 2006. Novel approaches to antimalarial drug discovery. Infect. Disord. Drug Targets 6, 173–204.

Bozdech, Z., Llinas, M., Pulliam, B.L., Wong, E.D., Zhu, J., DeRisi, J.L., 2003. The transcriptome of the intraerythrocytic developmental cycle of Plasmodium falciparum. PLoS Biol. 1 (1), E5.

Brady, R.L., Cameron, A., 2004. Structure-based approaches to the development of novel anti-malarials. Curr. Drug Targets 5, 137–149.

Campanale, N., Nickel, C., Daubenberger, C.A., Wehlan, D.A., Gorman, J.J., Klonis, N., Becker, K., Tilley, L., 2003. Identification and characterization of heme-interacting proteins in the malaria parasite, *Plasmodium falciparum*. J. Biol. Chem. 278, 27354–27361.

Colell, A., Ricci, J.E., Tait, S., Milasta, S., Maurer, U., Bouchier-Hayes, L., Fitzgerald, P., Guio-Carrion, A., Waterhouse, N.J., Li, C.W., Mari, B., Barbry, P., Newmeyer, D.D., Beere, H.M., Green, D.R., 2007. GAPDH and autophagy preserve survival after apoptotic cytochrome *c* release in the absence of caspase activation. Cell 129, 983–997.

Daubenberger, C.A., Poltl-Frank, F., Jiang, G., Lipp, J., Certa, U., Pluschke, G., 2000. Identification and recombinant expression of glyceraldehyde-3-phosphate dehydrogenase of *Plasmodium falciparum*. Gene 246, 255–264.

Daubenberger, C.A., Tisdale, E.J., Curcic, M., Diaz, D., Silvie, O., Mazier, D., Eling, W., Bohrmann, B., Matile, H., Pluschke, G., 2003. The N′-terminal domain of glyceraldehyde-3-phosphate dehydrogenase of the Apicomplexan *Plasmodium falciparum* mediates GTPase Rab2-dependent recruitment to membranes. Biol. Chem. 384, 1227–1237.

Dobeli, H., Trzeciak, A., Gillessen, D., Matile, H., Srivastava, I.K., Perrin, L.H., Jakob, P.E., Certa, U., 1990. Expression, purification, biochemical characterization and inhibition of recombinant *Plasmodium falciparum* aldolase. Mol. Biochem. Parasitol. 41, 259–268.

Fast, N.M., Kissinger, J.C., Roos, D.S., Keeling, P.J., 2001. Nuclear-encoded, plastid-targeted genes suggest a single common origin for Apicomplexan and Dinoflagellate plastids. Mol. Biol. Evol. 18, 418–426.

Foth, B.J., Ralph, S.A., Tonkin, C.J., Struck, N.S., Fraunholz, M., Roos, D.S., Cowman, A.F., McFadden, G.I., 2003. Dissecting apicoplast targeting in the malaria parasite *Plasmodium falciparum*. Science 299, 705–708.

Gille, C., Frommel, C., 2001. STRAP: editor for structural alignments of proteins. Bioinformatics 17, 377–378.

Gratzer, W., 1984. Cell biology. More red than dead. Nature 310, 368–369.

Guindon, S., Lethiec, F., Duroux, P., Gascuel, O., 2005. PHYML Online—a web server for fast maximum likelihood-based phylogenetic inference. Nucleic Acids Res. 33, W557–W559.

Hall, T., 1999. BioEdit: a user-friendly biological sequence alignment editor and analysis program for Windows 95/98/NT. In: Nucleic Acids Symposium Series [0261-3166], vol. 41. p. 95.

Jenkins, J.L., Tanner, J.J., 2006. High-resolution structure of human D-glyceraldehyde-3-phosphate dehydrogenase. Acta Crystallogr D Biol Crystallogr. 62 (Pt 3), 290–301.

Lakhdar-Ghazal, F., Blonski, C., Willson, M., Michels, P., Perie, J., 2002. Glycolysis and proteases as targets for the design of new anti-trypanosome drugs. Curr. Top. Med. Chem. 2 (5), 439–456 (Review).

Nagradova, N.K., 2001. Study of the properties of phosphorylating D-glyceraldehyde-3-phosphate dehydrogenase. Biochemistry 66, 1067–1076.

Newton, P., White, N., 1999. Malaria: new developments in treatment and prevention. Annu. Rev. Med. 50, 179–192.

Opperdoes, F.R., Michels, P.A., 2001. Enzymes of carbohydrate metabolism as potential drug targets. Int. J. Parasitol. 31 (5/6), 482–490 Review.

O'Sullivan, O., Suhre, K., Abergel, C., Higgins, D.G., Notredame, C., 2004. 3DCoffee: combining protein sequences and structures within multiple sequence alignments. J. Mol. Biol. 340, 385–395.

Rich, S.M., Ayala, F.J., 2003. Progress in malaria research: the case for phylogenetics. Adv. Parasitol. 54, 255–280.

Robien, M.A., Bosch, J., Buckner, F.S., van Voorhis, W.C., Worthey, E.A., Myler, P., Mehlin, C., Boni, E.E., Kalyuzhniy, O., Anderson, L., Lauricalla, A., Soltis, M., Zucker, F., Verlinde, C.L., Merritt, E.A., Schoenfeld, L.W., Hol, W.G., 2006. Crystal structure of glyceraldehyde-3-phosphate dehydrogenase from *Plasmodium falciparum* at 2.25A resolution reveals intriguing extra electron density in the active site. Proteins: Struct. Funct. Bioinform. 62, 570–577.

Roll Back Malaria (RBM) W.H.O., (WHO) a.U., 2005. World Malaria Report. pp. xvii.

Roth Jr., E., 1990. *Plasmodium falciparum* carbohydrate metabolism: a connection between host cell and parasite. Blood Cells 16, 453–460 (discussion 461-6).

Roth Jr., E.F., Calvin, M.C., Max-Audit, I., Rosa, J., Rosa, R., 1988. The enzymes of the glycolytic pathway in erythrocytes infected with *Plasmodium falciparum* malaria parasites. Blood 72, 1922–1925.

Satchell, J.F., Malby, R.L., Luo, C.S., Adisa, A., Alpyurek, A.E., Klonis, N., Smith, B.J., Colman, P.M., 2005. Structure of glyceraldehyde-3-phosphate dehydrogenase from *Plasmodium falciparum*. Acta Crystallogr. Sect. D 61, 1213–1221.

Sherman, I.W., 1998. Malaria: Parasite Biology, Pathogenesis, and Protection. ASM Press, Washington, DC.

Sirover, M.A., 1999. New insights into an old protein: the functional diversity of mammalian glyceraldehyde-3-phosphate dehydrogenase. Biochim. Biophys. Acta 1432, 159–184.

Waller, R.F., Keeling, P.J., Donald, R.G., Striepen, B., Handman, E., Lang-Unnasch, N., Cowman, A.F., Besra, G.S., Roos, D.S., McFadden, G.I., 1998. Nuclear-encoded proteins target to the plastid in *Toxoplasma gondii* and *Plasmodium falciparum*. Proc. Natl. Acad. Sci. U.S.A. 95, 12352–12357.

Wanidworanun, C., Nagel, R.L., Shear, H.L., 1999. Antisense oligonucleotides targeting malarial aldolase inhibit the asexual erythrocytic stages of *Plasmodium falciparum*. Mol. Biochem. Parasitol. 102, 91–101.